doi:10.1093/brain/awm045 *Brain* (2007), **130**, 1244–1253

Recovery from optic neuritis: an ROI-based analysis of LGN and visual cortical areas

Kirsten Korsholm,[1] Kristoffer H. Madsen,[1,2] Jette L. Frederiksen,[3] Arnold Skimminge[1,2] and Torben E. Lund[1]

[1]Danish Research Centre for Magnetic Resonance, Copenhagen University Hospital, Hvidovre, [2]Informatics and Mathematical Modelling, Technical University of Denmark, Lyngby and [3]Department of Neurology, Copenhagen University Hospital, Glostrup, Denmark

Correspondence to: Kirsten Korsholm, Danish Research Centre for Magnetic Resonance, Copenhagen University Hospital, Hvidovre, 2650 Hvidovre, Denmark
E-mail: kirstenk@drcmr.dk

Optic neuritis (ON) is the first clinical manifestation in ~20% of patients with multiple sclerosis (MS). The inflammation and demyelination of the optic nerve are characterized by symptomatic visual impairment and retrobulbar pain, and associated with decreased visual acuity, decreased colour and contrast sensitivity, delayed visual evoked potentials and visual field defects. Spontaneous recovery of vision typically occurs within weeks or months after onset, depending on the resolution of inflammation, remyelination, restoration of conduction in axons which persist demyelinated and neuronal plasticity in the cortical and subcortical visual pathways. To assess where recovery takes place along the visual pathway, visual activation was studied in the lateral geniculate nucleus (LGN), the main thalamic relay nucleus in the visual pathway and in three areas of the visual cortex: the lateral occipital complexes (LOC), V1 and V2. We conducted a longitudinal functional magnetic resonance imaging (fMRI) study of regions of interest (ROI) of activation in LGN and visual cortex in 19 patients with acute ON at onset, 3 and 6 months from presentation. With fMRI we measured the activation in the ROIs and compared activation during monocular stimulation of the affected and unaffected eye. In the acute phase the activation of LGN during visual stimulation of the affected eye was significantly reduced ($P < 0.01$) compared to the unaffected eye. This difference in LGN activation between the affected and unaffected eye diminished during recovery, and after 180 days the difference was no longer significant ($P = 0.59$). The decreased difference during recovery was mainly due to an increase in the fMRI signal when stimulating the affected eye, but included a component of a decreasing fMRI signal from LGN when stimulating the unaffected eye. In LOC, V1 and V2 activation during visual stimulation of the affected eye in the acute phase was significantly reduced ($P < 0.01$) compared to the unaffected eye, and during recovery the difference diminished with no significant differences left after 180 days. As the pattern of activation in LOC, V1 and V2 resembled the development in LGN we found no evidence of additional cortical adaptive changes. The reduced activation of the LGN to stimulation of the unaffected eye is interpreted as a shift away from early compensatory changes established in the acute phase in LGN and may indicate very early plasticity of the visual pathways.

Keywords: optic neuritis; lateral geniculate nucleus; lateral occipital complex (LOC); functional magnetic resonance imaging; regeneration

Abbreviations: LGN = lateral geniculate nucleus; LOC = lateral occipital complexes; MRI = magnetic resonance imaging; ON = optic neuritis; ROI = region of interest

Received October 24, 2006. Revised February 5, 2007. Accepted February 13, 2007

Introduction

Optic neuritis (ON) is the presenting symptom in ~20% of patients with multiple sclerosis (MS), the most common chronic disabling neurological disease in young adults (Sorensen *et al.*, 1999; Confavreux *et al.*, 2000). The 10-year risk of developing MS after isolated acute ON has been reported to ~40% (Ghezzi *et al.*, 1999; Beck *et al.*, 2003; Nilsson *et al.*, 2005). ON typically causes symptomatic visual impairment and retrobulbar pain developing over hours or days and is associated with decreased visual acuity, abnormal colour vision, decreased contrast sensitivity,

visual field defects such as central scotomas and delayed or broadened visual evoked potentials (VEP) (Frederiksen *et al.*, 1991). The pathophysiological mechanisms contributing to the clinical deficits in ON include inflammation, oedema, demyelination and axonal loss of the optic nerve (Smith and McDonald, 1999).

Within weeks or months after onset of symptoms, a spontaneous recovery of vision occurs and patients usually regain good vision. Many factors may contribute to the recovery process including resolution of inflammation, remyelination, restoration of conduction in persistently demyelinated axons (Smith and McDonald, 1999) and cortical or subcortical neuroplasticity (Werring *et al.*, 2000; Toosy *et al.*, 2002, 2005).

For studying recovery mechanisms in MS, ON is a useful model as the lesion is well-defined and can easily be assessed by clinical and electro-physiological tests. Magnetic resonance imaging (MRI) methods have proven particularly useful. Structural and diffusion weighted MRI have indicated atrophy of the optic nerve following ON (Iwasawa *et al.*, 1997; Hickman *et al.*, 2004, 2005; Trip *et al.*, 2006*b*), and a correlation between optic nerve atrophy and thinning of the retinal nerve fibre layer following ON suggests that the atrophy mainly is caused by axonal loss (Trip *et al.*, 2006*a*). In addition, it has been shown that despite a significant degree of optic nerve atrophy, a good recovery of visual acuity and visual field defects is possible, suggesting either redundancy of the anterior visual pathways or cortical remodelling of visual function (Hickman *et al.*, 2001).

Functional aspects of the repair mechanisms in ON and MS have been investigated using functional magnetic resonance imaging (fMRI), based on the blood oxygenation level dependent (BOLD) contrast (Ogawa *et al.*, 1990). These studies have focused on cortical changes following ON (Rombouts *et al.*, 1998; Gareau *et al.*, 1999; Werring *et al.*, 2000; Langkilde *et al.*, 2002; Russ *et al.*, 2002; Toosy *et al.*, 2002, 2005; Levin *et al.*, 2006). Patients with previous ON generally show decreased activation in visual cortex compared to controls (Rombouts *et al.*, 1998; Gareau *et al.*, 1999; Werring *et al.*, 2000; Toosy *et al.*, 2002; Langkilde *et al.*, 2002). Abnormal extra-occipital activation has also been reported following ON (Werring *et al.*, 2000; Toosy *et al.*, 2002), and recently cortical adaptive changes following ON have been reported to occur in the lateral occipital complexes (LOC) (Toosy *et al.*, 2005; Levin *et al.*, 2006). Toosy *et al.* reported adaptive changes in LOC in the acute phase of ON. In contrast, Levin *et al.* suggested that the LOC is robust to disruptions of the visual input, as they find normal activation in LOC upon stimulation of the affected eye as opposed to decreased activation in early visual areas in their population of patients at various stages of ON.

However, it is unresolved to what extent the changed BOLD signal in visual cortex reflects altered cortical reactivity or merely an increased input from a recovered optic nerve (Russ *et al.*, 2002). Presently in ON, the role of the lateral geniculate nucleus (LGN), the main thalamic relay nucleus in the visual pathway, remains controversial: The optic nerve might remyelinate sufficiently to re-establish a normal input to the LGN and with this a normal input to the primary visual cortex, or the LGN might compensate for an impaired optic nerve input and in this way provide a normal input to the primary visual cortex. However, if input from LGN to the primary visual cortex is impaired then adaptive changes in early or higher visual areas might assist in maintaining normal visual function (Faro *et al.*, 2002).

We hypothesized that recovery processes located in the optic nerve will be reflected as increased activation already at the level of LGN during recovery.

LGN function can be mapped with fMRI during visual stimulation (Chen *et al.*, 1998, 1999; Kastner *et al.*, 2004). One case-study of fMRI-activation in LGN in a patient with acute ON reported bilateral LGN activation during stimulation of the healthy eye, whereas stimulation of the affected eye in the acute phase yielded no LGN activation (Miki *et al.*, 2003). This suggests that measurements of LGN activation with fMRI can be used for monitoring optic nerve function.

In the present study, we examined 19 patients at presentation of ON and again after 2 weeks, 3 months and 6 months. We assessed the BOLD fMRI activation in the two LGN comparing the signal during monocular stimulation of the affected and the unaffected eye, in order to test the hypothesis that recovery of optic nerve function and LGN plasticity can account for the clinical recovery from ON. In addition, we used a region of interest (ROI) approach in LOC, V1 and V2 to study the relationship between LGN activation and activation of these visual areas.

Material and methods

Patients

Twenty-three consecutively referred patients with acute ON were included in the study. One patient was excluded during the study due to excessive sleepiness in the scanner, and three patients withdrew after the first, second and third examinations respectively. The remaining 19 patients (15 women, 4 men, median age 31.5 years, range 18–45 years) had either clinically isolated acute ON (14 patients) or acute ON as part of relapsing remitting multiple sclerosis (RRMS: 5 patients). Patients with RRMS were eligible for the study as long as this was their first presentation with ON and the latency of the visual evoked potential (VEP) of their unaffected eye was within normal values ($\leqslant$112 ms) at the time of inclusion.

The median duration of the acute ON at the time of the first MRI was 19 days (range 9–42 days). Detailed clinical information on each patient can be found in Table 1.

The diagnosis of ON was verified by clinical examination and para-clinical testing comprising visual acuity, contrast sensitivity and colour vision testing with Ishihara pseudo-isochromatic plates number 1–25, autoperimetry and VEP. These were repeated prior to each MRI examination. The patients were examined in the acute phase, and three serial follow-up examinations were

Table 1 Clinical characteristics of the patients

Patient #	Sex	Age	Affected eye	Snellen VA (AE)	Snellen VA (UE)	Diagnosis	Days from onset to inclusion
1	F	37	R	CF/1.0/1.0/1.0	1.0/1.0/1.0/1.0	ON & RRMS	20
2	F	27	R	HM/0.4/1.0/0.9	0.9/0.8/1.0/0.8	ON	13
3	F	31	L	0.6/0.7/0.7/0.8	1.0/1.0/1.0/1.0	ON & RRMS	9
4	M	36	L	CF/0.6/0.9/1.0	1.0/1.0/1.0/1.0	ON	37
5	F	21	R	CF/1.0/0.7/1.0	1.0/1.0/1.0/1.0	ON	17
6	F	31	L	S/HM/CF/1.0	1.0/1.0/1.0/1.0	ON	13
7	F	18	L	CF/1.0/1.0/1.0	1.0/1.0/1.0/1.0	ON	9
8	F	22	R	0.4/NLP/0.5/0.9	1.0/1.0/1.0/1.0	ON	18
9	M	27	R	HM/CF/0.2/0.4	0.6/0.6/0.8/0.6	ON	16
10	M	41	L	0.4/1.0/0.9/1.0	1.0/1.0/1.0/1.0	ON	19
11	F	32	R	0.4/0.5/0.7/0.3	0.8/0.8/0.8/0.9	ON	25
12	F	37	R	1.0/1.0/1.0/1.0	1.0/1.0/1.0/1.0	ON & RRMS	42
13	F	25	L	0.1/0.5/1.0/1.0	1.0/1.0/1.0/1.0	ON	16
14	F	34	R	0.3/0.5/0.5/0.6	0.9/0.9/0.9/0.9	ON	20
15	F	44	L	0.6/0.9/1.0/1.0	1.0/1.0/1.0/1.0	ON	21
16	M	31	L	1.0/1.0/1.0/1.0	1.0/1.0/1.0/1.0	ON & RRMS	28
17	F	45	L	0.1/1.0/1.0/1.0	0.8/0.9/1.0/1.0	ON	22
18	F	32	L	0.5/0.7/1.0/1.0	1.0/1.0/1.0/1.0	ON	20
19	F	20	L	CF/0.7/0.8/0.8	1.0/1.0/1.0/1.0	ON & RRMS	11

F = female; M = male; R = right; L = left; VA = visual acuity; AE = affected eye; UE = unaffected eye; ON = optic neuritis; RRMS = relapsing remitting multiple sclerosis. VA is shown for first, second, third and fourth examination. CF = counting fingers; HM = hand movements; S = silhouette (patients able to silhouette of a person standing 1 m away); NLP = no light perception; Comment: Patient no. 5 develops RRMS after inclusion.

performed 2 weeks, 3 months and 6 months after the acute phase examination.

The study was approved by the local scientific ethics committee (protocol no. KF 01-115/04) and written informed consent was obtained from all the subjects in accordance with the Helsinki Declaration.

Visual tests

Visual acuity (VA) was assessed monocularly by the Snellen chart at 6 m. To test for significant differences between VA of the affected and unaffected eye at the fourth examination we used a Mann–Whitney test.

Autoperimetry of the central 30° region of the visual field was performed with a Humphrey Field Analyzer on each eye. Scotomas covering the central 5° of vision or more were classified as central scotomas.

The effect of time on Humphreys Mean Deviation (HMD) of the affected and unaffected eye was assessed using a least squares linear regression with respect to disease duration, and the significances of the slopes were tested with a one-sided *t*-test for the affected eye and a two-sided *t*-test for the unaffected eye.

Monocular VEPs were recorded with whole-field (27°), pattern-reversal chequerboards (9 mm). The amplitude and the latency of the major positive component (P100) were measured. The effect of time on VEP latencies and on VEP amplitudes of the affected eye and unaffected eye was investigated using a least squares linear regression with respect to disease duration. The significances of the regression slopes were assessed using a one-sided *t*-test for the affected eye and a two-sided *t*-test for the unaffected eye. To illustrate trends over time for the visual tests, windowed averages were calculated using a Gaussian window with full-width at half maximum (FWHM) of 100 days (Figures S6 and S7) (supplementary material).

MRI

The MRI included a functional scan followed by a structural scan on a 3.0 T Siemens Magnetom Trio Scanner (Siemens, Erlangen, Germany).

Structural images

Structural images, used for drawing of ROI and for diagnosis, were acquired with an eight-channel head coil (Invivo, FL, USA) and included:

(1) MPRAGE (magnetization prepared rapid acquisition gradient echo) with a voxel dimension of $1 \times 1 \times 1\,mm^3$, field of view (FOV) 256 mm, matrix 256×256, repetition time(TR)/echo time(TE)/inversion time (TI) = 1540/3.93/800 ms and a flip-angle of 9°, before and after a double dose of paramagnetic contrast-agent (0.2 mmol/kg Magnevist, 0.5 mmol/ml, Schering AG, Berlin).
(2) Axial FLAIR (fluid attenuated inversion recovery) images: 42 slices with a thickness of 3 mm, FOV 230 mm, matrix 256×256, TR/TI/TE = 9000/2400/85 ms and a flip-angle of 150°.
(3) Axial turbo spin echo (TSE), 42 slices with a thickness of 3 mm, FOV 230 mm, matrix 256×252, TR/TE1/TE2 = 8820/115/14 ms and a flip-angle of 163°.

Functional MRI

The functional MRI was acquired with a standard single channel birdcage head coil (Siemens, Erlangen, Germany). In order to position the functional scan correctly an MPRAGE volume was also acquired with the standard single channel birdcage head coil prior to the functional scan. T2*-weighted echo planar imaging (EPI), with 42 slices of 3 mm, positioned parallel to the calcarine

sulcus, were acquired with the following parameters: TR = 2.49 s, TE = 30 ms, flip-angle 90°, FOV 192 mm and in-plane resolution $3 \times 3 mm^2$. For each eye 121 volumes were acquired. During the functional MRI acquisition the cardiac cycle and the respiratory rate were recorded with an infrared pulse oximeter on the patient's index-finger and a pneumatic thoracic belt, respectively.

Experimental procedure

Visual stimulation was provided by means of a LCD projector (Canon LV7540), located outside the scanner room, and a zoom lens (Buhl Optics 849MCZ087) projected the image through a wave-guide onto a screen behind the patient's head. The screen covered 12° × 18° of the visual field and was visible to the patient through a mirror mounted on the head coil.

During the fMRI session the scanner room was darkened. The patient viewed a stimulus consisting of a full-field black and white circular chequerboard reversing at 8 Hz with chequers of sizes reflecting the cortical magnification factor (Slotnick *et al.*, 2001). Each eye was stimulated separately (block design, 10 s of flickering chequerboard, 10 s pause, total scan time per eye 5 min 6 s), the other eye was covered by an eye-pad. When changing the eye-pad to the other eye, the patient was not removed from the head coil. We balanced the sequence in which the affected or the unaffected eye was stimulated, that is, half of the patients had their unaffected eye stimulated first. This order was kept for subsequent examinations.

A fixation dot remained throughout the experiment and this randomly changed colour from red to green (with a random interval of 4–8 s, the colour green remaining for 500 ms). To maintain attention to the central visual stimulus subjects 7 to 19 were asked to press a button each time the colour of the fixation dot changed. At inclusion, all patients were able to at least perceive light, and all patients could as such participate in the visual stimulation fMRI paradigm. However, in the acute phase some of the patients had central scotomas impairing central fixation. They were instructed to keep their eye open and to look at the centre of the screen, guided by peripheral visual cues including the circular chequerboard.

To assess the effect of time on the attentional task performances, a linear regression was performed for both the affected and unaffected eye with respect to disease duration, and the significances of the slopes were tested with a one-sided *t*-test for the affected eye and a two-sided *t*-test for the unaffected eye.

ROI construction

LGN

The LGN is ~$5 \times 6 \times 9 mm^3$ (Horton *et al.*, 1990; Saeki *et al.*, 2003). To minimize partial volume effects due to this small size we delineated LGN on 3D T1-weighted images (MPRAGE) according to the published landmarks (Horton *et al.*, 1990; Tamraz, 1994) using 'DISPLAY' (http://www.bic.mni.mcgill.ca/). The delineation procedure is described in Fig. S1 (supplementary material). ROIs were drawn on MPRAGEs from the first and the third scan of each patient. If an adequate MPRAGE image from first or third examination was missing, the second or fourth was used instead. The union of the ROIs from the first and third scan was used for further analysis.

After ROI-drawing on the MPRAGE images, the EPI images were motion corrected and registered to the first same-session EPI. The EPI images were then registered (mutual information) to the same-session MPRAGE using a six parameter rigid body transformation and subsequently this was registered to the MPRAGE of the first examination. Finally the transformations were applied to the EPI images and the LGN ROIs from the respective examinations. All registrations were done using SPM2 (http://www.fil.ion.ucl.ac.uk/spm/).

A two-sided paired *t*-test was used to test for differences between LGN-volumes of the first and third scan.

LOC, V1 and V2

An ROI-based approach was applied to study the activation in LOC, V1 and V2. EPI images were spatially normalized using SPM2 (with default settings) to the SPM2 EPI template in Montreal Neurological Institute (MNI) space. The normalized EPI images were smoothed with a Gaussian filter with a FWHM of 8 mm (smoothing is beneficial when analysing ROIs in standard space to reduce inter-subject variability due to imperfect spatial normalization).

As the hypothesis on adaptive changes in LOC had not evolved when our study was initiated a localizer task for LOC was not included in our paradigm. Instead LOC was defined as two bilateral spheres with a volume of ~$1 cm^3$ centred around the average reported MNI coordinates of the LOC in a previous study (±43, −70, −13) (Toosy *et al.*, 2005).

Differences in scotoma location between patients make a voxel-wise group analysis of primary and secondary visual cortices problematic. For this reason we restricted ourselves to an ROI analysis also in these areas. Thus, V1 and V2 were defined as BA17 and BA18 from the probabilistic cyto-architectonic maps (Wohlschlager *et al.*, 2005) in the SPM Anatomy Toolbox (Eickhoff *et al.*, 2005).

Data analysis

Statistical analysis of fMRI data was performed using a general linear model where the signal of interest was modelled as a box car convolved with the standard SPM2 canonical haemodynamic response function. Serial correlations were modelled using a nuisance variable regression approach. For a thorough review of this procedure see Lund *et al.*, 2006. In addition to the SPM2 standard discrete cosine set high pass filter (128 s cut off), this approach consists of regressors based on cardiac and respiratory oscillations and expanded motion parameters included in the design matrix. Regarding LGN, after model estimation, the effect size maps were re-sliced using nearest neighbour interpolation to match the resolution of the structural images, and thereby the ROIs.

To accommodate non-motion session effects (caffeine intake, menstrual cycle, etc.) we calculated for each examination within each ROI, the average BOLD signal change (amplitude) for all voxels included in the ROI during stimulation of the affected and the unaffected eye and the difference between the affected and the unaffected eye.

The effect of time was investigated using a least squares linear regression of the activation in each ROI during stimulation of the affected and unaffected eye and the difference between them with respect to disease duration. The significances of the regression slopes were then assessed using a one sided *t*-test for the affected eye and for the difference between the two eyes. To test the significance of the slope for the unaffected eye a two-sided *t*-test was used. Furthermore, to illustrate trends, windowed averages

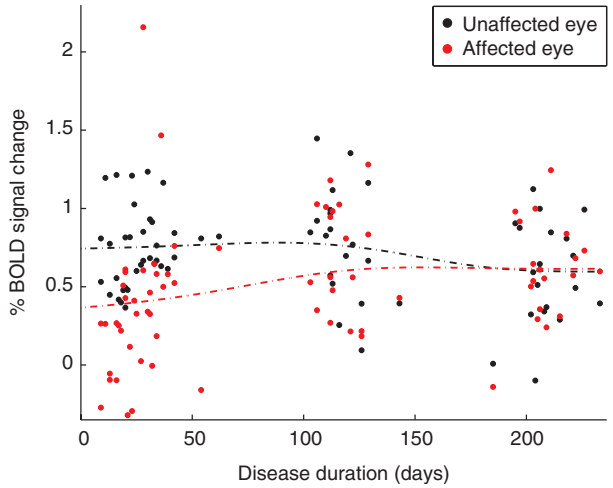

Fig. 1 Mean LGN activation during stimulation of the affected and unaffected eye over time. The dash-dotted lines indicate weighted moving averages (Gaussian window with full width at half maximum of 100 days) for the affected eye (red) and unaffected eye (black). During recovery there is a significant increase in LGN BOLD signal from stimulation of the affected eye (one-sided *t*-test of regression slope: $t = 2.51$, df = 71, $P < 0.01$). The LGN BOLD signal from stimulation of the unaffected eye decreases over time in a stepwise fashion. *Post hoc* testing showed this decrease to be significant (two sample *t*-test with measurements before 180 days in group 1 and later measurements in group 2: $t = 2.18$, df = 71, $P = 0.02$). It is seen that the BOLD signal changes for the affected and unaffected eye level off at a similar positive level as time increases.

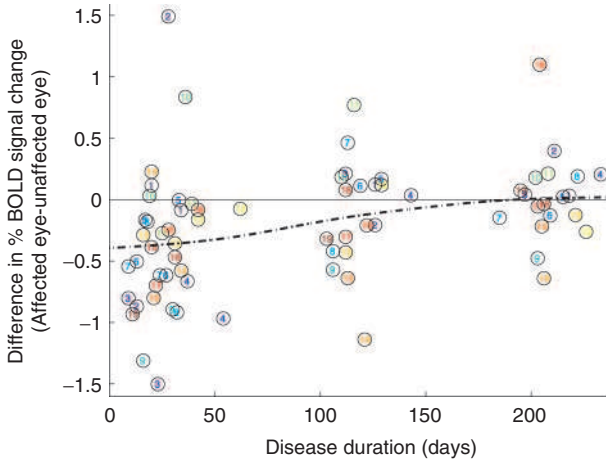

Fig. 2 Difference in LGN activation between the affected and the unaffected eye over time. Each patient has his/her own coloured number corresponding to patient number in Table 1. The dash-dotted line indicates a weighted moving average (Gaussian window with full width at half maximum of 100 days). It is seen that the difference in LGN BOLD signal change between the affected and unaffected eye approaches zero as time increases. The effect of time was assessed using a least squares linear regression. Using a one-sided *t*-test the regression slope was found significant ($t = 3.23$, df = 71, $P < 0.01$).

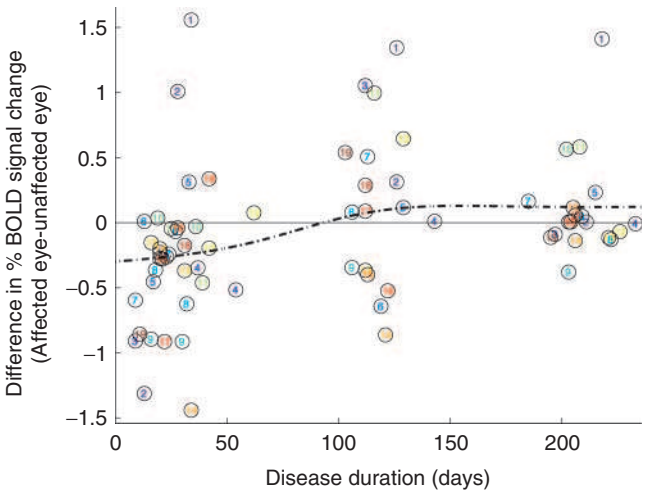

Fig. 3 Difference in activation in LOC between the affected and the unaffected eye over time. Each patient has his/her own coloured number corresponding to patient number in Table 1. The dash-dotted lines indicate weighted moving averages (Gaussian window with full width at half maximum of 100 days). It is seen that the difference in BOLD signal changes in LOC between affected and unaffected eye decreases significantly during recovery. The effect of time was assessed using a least squares linear regression. Using a one-sided *t*-test the regression slope was found significant ($t = 3.01$, df = 70, $P < 0.01$).

were calculated using a Gaussian window with a FWHM of 100 days. These trend-lines are shown in Figs 1, 2, 3, S3, S4 and S5.

The difference in activation between affected and unaffected eye in the acute phase was tested using a paired *t*-test on all pairs of measurements collected before day 50. Also using a paired *t*-test, the difference after recovery was assessed using all pairs of measurements collected after day 180.

Least squares linear fit between ROI BOLD signal changes and HMD, VEP latency and VEP amplitude of the affected eye were performed and the regression slopes were tested with a one-sided *t*-test. For all tests a *P*-value below 0.05 was considered significant.

The TSE and FLAIR images were co-registered to the MPRAGE of the same session, and all abnormalities localized to the retrochiasmal pathways were noted (Miller, 1982).

Results

Neuro-ophthalmological testing

Patient information including diagnosis and VA of the affected and unaffected eye are listed in Table 1. The changes in VA from the first to the fourth examination are visualized in Fig. S2 (supplementary material). It is seen that the majority of patients' VA have normalized at the time of the fourth examination, and at the fourth examination no significant difference between VA of the affected and unaffected eye was found ($P = 0.34$).

In Fig. S6 (A) (supplementary material) the VEP latencies for the affected (red dash dotted line) and unaffected (black dash dotted line) eye are shown as a function of disease duration. It is seen that the prolonged VEP latency of the affected eye remained relatively unchanged during the 6 months of examination, and test of the regression slope was non-significant ($t = 0.80$, df = 56, $P = 0.21$). For the

unaffected eye no significant change in VEP latency was found over time ($t = 1.65$, df = 68, $P = 0.10$). In Fig. S6 (B) (supplementary material) VEP amplitudes for the affected and unaffected eye are shown as function of disease duration. VEP amplitudes of the affected eye increased significantly over time ($t = 2.07$, df = 56, $P = 0.02$), while VEP amplitudes of the unaffected eye remained relatively stable with no significant effect of time ($t = 0.51$, df = 68, $P = 0.61$).

HMD are listed in Table S1 (supplementary material) together with data on central scotomas and fMRI performance. Nine out of 19 patients had central scotomas of the affected eye at first examination, and three patients (no. 7, 18 and 19) had partial central scotomas. None had scotomas covering central vision by the third examination.

In Fig. S7 (supplementary material) HMD of the affected and unaffected eye are shown as a function of disease duration; it is seen that the HMD of the affected eye increases over time ($t = 4.60$, df = 70, $P < 0.01$). For the unaffected eye HMD remains relatively stable ($t = 1.74$, df = 69 $P = 0.08$).

The mean target detection rate during all fMRI examinations of the unaffected eye was 94.7%, and did not change significantly over time ($t = -0.54$, df = 47, $P = 0.58$). The performance during stimulation of the affected eye was impaired at onset (mean detection rate: 55.9%) and increased significantly over time ($t = 3.06$, df = 47, $P < 0.01$) approaching values of the unaffected eye at the fourth examination (mean detection rate: 85.8%).

When stimulating the unaffected eye none of the patients had more than one lost target in a row. When stimulating the affected eye none of the patients who did not have a central scotoma had more than four misses in a row.

Structural MRI

The overall mean volume of the delineated LGN (averaged over left and right and the two examinations of the 19 subjects) was 267 mm^3 with a between-subject standard deviation of 27 mm^3. With the resolution used, the volume of LGN corresponds to approximately 10 EPI voxels with one voxel standard deviation between subjects. Testing with a two-sided paired t-test, no significant changes in LGN volumes from the acute scan (mean 266 mm^3) to the 3 months scan (mean 269 mm^3) were found ($t = -0.39$, df = 18, $P = 0.70$).

Overall, at inclusion 8 of the 19 patients had small hyperintense lesions in the optic radiations (OR), and at the end of the study 9 of the 19 patients had hyperintense lesions in the OR. In the acute phase, three patients had gadolinium-enhancing lesions in the OR, which had ceased by 3 months. None of the patients developed new gadolinium-enhancing lesions in the OR after the second scan, and one patient developed a new white-matter lesion in the OR during the study.

Functional MRI

LGN

The results of the LGN ROI analysis of the fMRI data are summarized in Figs 1 and 2. When stimulating the unaffected eye we obtained a positive BOLD fMRI-response from the region of interest (union of both LGNs) [Fig. 1, black dash dotted line, and Fig. S3 (B) (supplementary material)]. The test of the regression slope of a linear change with time was non-significant (two-sided t-test: $t = -1.66$, df = 71, $P = 0.10$). From the figure it is, however, seen that the LGN activity when stimulating the unaffected eye seems to decrease in a stepwise fashion, with the lower level starting around day 180. *Post hoc* testing showed this decrease to be significant (two sample t-test with measurements before 180 days in group 1 and later measurements in group 2: $t = 2.18$, df = 71, $P = 0.02$).

The BOLD signal obtained when stimulating the affected eye in the acute phase (<50 days) was also positive (one-sided t-test: $t = 4.47$, df = 32, $P < 0.01$). During recovery there was a significant increase in LGN BOLD signal from stimulation of the affected eye (one-sided t-test of regression slope: $t = 2.51$, df = 71, $P < 0.01$) [Fig. 1 red dash dotted line and Fig. S3 (A) (supplementary material)].

In the acute phase (<50 days from onset), the difference between the BOLD fMRI-responses obtained from LGN during stimulation of the affected eye and the unaffected eye, was statistically significant (one-sided paired t-test on measurements before day 50: $t = -3.77$, df = 32, $P < 0.01$) (Fig. 2). During recovery the difference between the affected and unaffected eye decreased significantly (one-sided t-test of regression slope: $t = 3.23$, df = 71, $P < 0.01$) (Fig. 2). After recovery the curves for the affected and unaffected eye seem to flatten out and meet at the same positive level, and after 180 days the BOLD signals in LGN from the affected and unaffected eye are no longer significantly different (one-sided paired t-test on measurements after day 180: $t = 0.23$, df = 18, $P = 0.59$) (Fig. 1).

LOC, V1 and V2

Positive BOLD fMRI-responses were observed across all subjects in all ROIs during stimulation of the affected and unaffected eye at all four examinations (supplementary Fig. S5).

In the acute phase the differences between the BOLD fMRI-responses obtained during stimulation of the affected eye and the unaffected eye were statistically significant with less activation from the affected eye (one-sided paired t-test on measurements before day 50) in LOC ($t = -2.81$, df = 32, $P < 0.01$) (Fig. 3), in V1 ($t = -2.89$, df = 32, $P < 0.01$) and in V2 ($t = -2.86$, df = 32, $P < 0.01$) (Fig. S4) (supplementary material).

During recovery the difference between the affected and unaffected eye decreased significantly (one-sided t-test of regression slope) in LOC ($t = 3.01$, df = 70, $P < 0.01$),

in V1 ($t=3.02$, df$=70$, $P<0.01$) and in V2 ($t=3.23$, df$=70$, $P<0.01$), and after recovery (after day 180) the differences in mean BOLD signal between stimulation of the unaffected and the affected eye in each area (LOC, V1 and V2) were no longer significantly different (Fig. 3 and S4).

Clinically isolated ON versus RRMS

No significant differences in activation were seen between patients with clinically isolated ON and patients with RRMS in either LGN or LOC. However, in V1 and V2 the differences between affected and unaffected eyes were significantly more pronounced for patients with clinically isolated ON than for patients with RRMS (two-sided two sample *t*-test on measurements before day 50: V1: $P=0.03$, V2: $P=0.03$).

Correlation between BOLD and neuro-ophthalomological visual tests

While both VEP amplitude and BOLD LGN activity of the affected eye increased over time, no significant correlation between the two measures was found. Neither did we find a correlation between VEP latency and BOLD LGN activity of the affected eye. Significant correlations were found between VEP amplitude and BOLD activity of the affected eye in LOC, V1 and V2 (LOC: $t=2.82$, df$=56$, $P<0.01$, V1: $t=2.93$, df$=56$, $P<0.01$, V2: $t=2.69$, df$=56$, $P<0.01$). No significant correlations were found between VEP latency and BOLD activity of the affected eye in LOC, V1 and V2.

A significant correlation with HMD was found for both VEP amplitude (data not shown) and BOLD signal from LGN of the affected eye. In Fig. 4 we have plotted, for the affected eye, the BOLD signal change in LGN as a function of HMD. The BOLD-signal is seen to increase with increasing HMD (one-sided *t*-test of regression slope: $t=3.85$, df$=70$, $P<0.01$). Significant correlations between HMD and BOLD activation of the affected eye were also found for LOC, V1 and V2 (LOC: $t=3.71$, df$=70$, $P<0.01$, V1: $t=5.12$, df$=70$, $P<0.01$, V2: $t=5.16$, df$=70$, $P<0.01$).

Discussion

This is the first systematic longitudinal analysis of the role of the LGN during recovery from acute ON. We confirm that fMRI is a suitable tool for measuring functional activation in the LGN (Chen *et al.*, 1998, 1999; Kastner *et al.*, 2004; Schneider *et al.*, 2004), including patients (Miki *et al.*, 2001, 2003, 2005). In contrast to previous studies, in which LGN was located based on statistical maps of the functional images superimposed on structural images (Miki *et al.*, 2001, 2003, 2005), we delineated LGN on structural images in advance of analysing the functional images. Using this ROI-based analysis, we were able to resolve LGN from adjacent structures such as the pulvinar, where activation also can be demonstrated during visual stimulation (Chen *et al.*, 1998; Kastner *et al.*, 2004). In addition, we investigated the activation in LOC, V1 and V2 using a standard space ROI-based approach.

We also used VEP to assess electrophysiological recovery of visual function. In acute ON, the VEP latency is usually prolonged and the amplitude is decreased, and typically, amplitude increases with clinical recovery, but latency may or may not recover (Halliday *et al.*, 1972; Jones, 1993; Frederiksen and Petrera, 1999; Brusa *et al.*, 1999, 2001). In our patients the mean amplitude of the VEP signal from the affected eye increased during recovery, but the latency remained prolonged suggesting that significant remyelination had not taken place by 6 months. This dissociation between recovery of latency and amplitude points to early recovery of conduction before re-myelination is established.

With fMRI, in the acute phase of the disease we found that the average BOLD signal changes in LGN, induced by monocular stimulation of the affected eye, were reduced compared to the unaffected eye. The reduced activation of the LGN in the acute phase is probably caused by reduced neuronal input to the LGN due to inflammation, oedema and demyelination of the optic nerve (Smith and McDonald, 1999) consistent with reduced VEP amplitudes and prolonged VEP latencies.

The increased LGN activation during recovery when stimulating the affected eye, may in part be due to restoration of conduction through the optic nerve, as the inflammation and oedema resolve during the first months (Youl *et al.*, 1991). This is consistent with an increase in VEP amplitudes during recovery. The persistently delayed VEP latencies in our subjects (Fig. S6) (supplementary

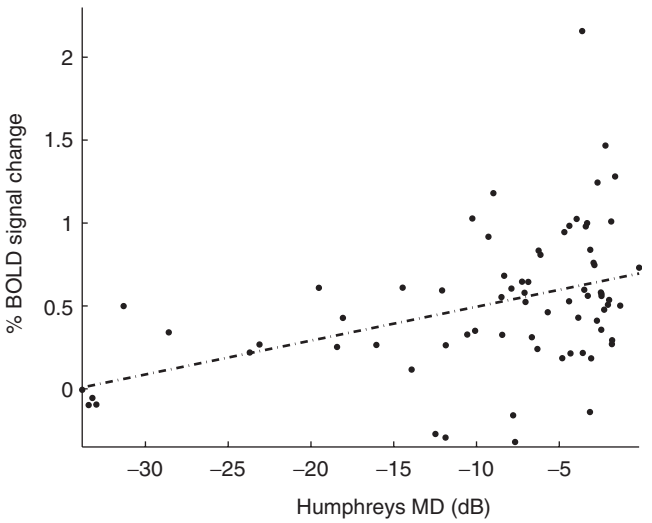

Fig. 4 Humphreys mean deviation (HMD) versus percent BOLD signal change (affected eye). The dash-dotted line show a least squares linear fit of HMD of the affected eye and percent BOLD signal change in LGN during stimulation of the affected eye. The BOLD-signal is seen to increase with increasing HMD (one-sided *t*-test of the regression slope: $t=3.85$, df$=70$, $P<0.01$).

material) and in previous reports (Halliday *et al.*, 1972) suggest that remyelination is not the primary mechanism of recovery of the LGN activation.

When stimulating the unaffected eye we saw a stepwise decrease in LGN activity over time. This effect was significant when comparing LGN activity before and after 180 days, the largest difference taking place between day 120 and 180. We suggest that this is due to a compensatory mechanism elicited by the unaffected eye, or the LGN itself, in the acute phase, where the vision of the affected eye was poor. As vision on the affected eye normalizes this compensatory mechanism gradually disappears. This is consistent with what is found in studies of motor activation in patients with MS where patients exhibit more activation in motor areas during a simple motor task than healthy controls suggesting that compensatory mechanisms help to restore function after functional disabilities (Pantano *et al.*, 2002; Rocca *et al.*, 2003). In addition, this compensatory activation is seen to normalize in younger patients with MS during periods without active disease (Pantano *et al.*, 2005). It is, however, possible that it reflects an early attentional effect, with the patient paying less attention to the stimulus during the last examination. Although such attentional modulation of LGN has been demonstrated electrophysiologically and with fMRI (O'Connor *et al.*, 2002; McAlonan *et al.*, 2006), our task performance data do not support this interpretation as the performance of the unaffected eye did not change significantly over time. It could also be argued that the decreased activation of LGN of the unaffected eye was due to asymptomatic ON during the 6-month follow-up period, however, our visual data do not support this.

In LOC, V1 and V2 the BOLD signal changes induced by monocular stimulation of the affected eye in the acute phase were significantly reduced compared to the unaffected eye. During recovery this difference between eyes disappeared. As this pattern matches the evolution of changes in LGN our data do not provide evidence for additional adaptive mechanisms in cortex. Thus, we cannot support the hypothesis by Levin *et al.* (2006) that LOC should be inherently robust to disruptions of the visual input in the acute phase. In contrast, in the acute phase we found a significant difference in activation in LOC between stimulation of the affected and the unaffected eye which was absent after recovery.

However, it could be argued that cortical adaptive changes are primary and that backprojection to LGN from visual cortices causes LGN to follow the cortical pattern. In fMRI studies of LGN activation in patients with visual disturbances, LGN activation has been found to be diminished in patients with both pre-geniculate and chronic post-geniculate lesions (Miki *et al.*, 2001, 2003, 2005). Reduced LGN activation ipsilateral to a retrogeniculate lesion could be an effect of retrograde degeneration of LGN or an effect of interrupted top–down projection to LGN from the visual cortex (Miki *et al.*, 2005). The top–down inputs, that LGN receive from the visual cortex, control the flow of information to the visual cortex by modulating the responsiveness and excitability of the geniculate cells, and these projections could be affected by lesions in the optic radiations and cause diminished LGN activation (Sherman, 2005).

By separating the eight patients with OR lesions from the 11 patients without lesions and calculating a lateralization index of number of plaques in the left/right OR, we tried to determine if LGN activation was influenced by back-projection from visual cortex. If backprojection to LGN from visual cortex was influenced by lesions in the OR, then lesions in the left OR would affect the activation in the left LGN and thereby reduce this compared to the activation of the right LGN, if there were no lesions in the right OR. However, when comparing left and right LGN activation in the patients with unequal number of lesions in the left and right OR, we found no differences in LGN activation, neither when comparing left and right LGN activation during stimulation of the unaffected eye, nor during stimulation of the affected eye. However, this *post hoc* analysis is underpowered due to the low numbers of patients with concurrent unilateral OR lesions. Thus, cortical adaptation might be primary, although we believe that our data are most suggestive of primary LGN changes in response to optic nerve recovery.

Partial volume effects and atrophy are potential confounding factors. The delineated LGNs had a mean volume of 267 mm^3 (corresponding to approximately 10 of our EPI voxels) with an intersubject standard deviation of 27 mm^3. In anatomical studies, LGN is found to be $\sim 5 \times 6 \times 9\ mm^3$ (Horton *et al.*, 1990; Saeki *et al.*, 2003). Other studies of autopsies report mean volumes of 120 mm^3, however, with a 2–3-fold variation between individuals (Andrews *et al.*, 1997). Although our volumes are in agreement with reported volumes, it is difficult in MRI to completely avoid partial volume effects when delineating such small structures. For our ROI-based fMRI analysis we used the union of ROIs drawn on sessions separated by 3 months. To assess the specificity of the drawn ROIs we repeated the analysis with two other approaches of constructing the ROI. The first approach included only voxels outlined in both drawings of LGN (the intersection of the ROIs), the second included voxels only outlined once (the complement). As our results remained largely unchanged when using the intersection of the two ROIs (first approach), we do not think that our results are largely contaminated by partial volume effects. When using the second approach where more 'edge' area and larger partial volumes effects are expected, the significance was reduced, indicating high specificity of our drawn ROIs.

Also in LOC it is difficult to avoid partial volume effects when applying a small ROI to brains normalized to standard space. By calculating the difference in average BOLD signal change between the two eyes for all voxels included in the LOC ROI partial volume effects are reduced. Even though we did not use a dedicated LOC

localizer task, we did find an appropriately positive BOLD signal in the LOC ROI across all subjects.

In V1 and V2, but not in LGN and LOC, the differences in activation between stimulation of the affected and unaffected eyes were significantly more pronounced for patients with clinically isolated ON than for patients with RRMS. It is unclear why MS patients show less differences between affected and unaffected eyes, however, the overall findings are not driven or compromised by the RRMS patient group.

One potential weakness of our study is that some of the patients in the acute phase had difficulties focusing on the central colour point of the flickering chequerboard with the affected eye. To solve this problem, we considered using an eye-tracker, but calibration would also be difficult to validate because of the central scotoma. Instead we instructed the patients, who had central scotomas, to look in the middle of the chequerboard guided by the circular flickering chequerboard, and none of the patients reported problems doing this.

Patients with poor performances in the initial phase all had central or partial central scotomas. Among these, we found three different subjects who performed better during rest than during flickering chequerboard; this is probably due to the fact that it is easier to see a dot changing colour on a non-flickering background. Thus for first time examination of patients 7, 17 and 18 the relative poor performance reported in Table S1 (supplementary material) does not necessarily reflect lack of attention which is supported by the positive BOLD signal observed in those subjects. Also performance data, when stimulating the unaffected eye, suggest that the same patients were attending as required.

In the current study the patients had to come back three times, so to increase patient compliance we kept the scanning time as short as possible and hence we did not include dedicated structural images of optic nerve integrity. Future studies could include both imaging markers of the structural integrity of the optic nerve and fMRI of LGN activation to investigate the relationship between the two.

Conclusion

During recovery from an episode of acute ON the activation in LGN elicited by stimulation of the affected eye, returns to the same level as that of the unaffected eye. This pattern is also seen in LOC, V1 and V2. In addition, we also find evidence for acute supra-normal compensatory changes following stimulation of the unaffected eye in LGN supporting theories on plastic changes in the adult brain during disease.

Supplementary material

Supplementary material is available at *Brain* Online.

Acknowledgements

The Simon Spies Foundation is acknowledged for donation of the Siemens Trio scanner. This study was supported by grants from the Danish Multiple Sclerosis Society. We would also like to thank Dr James Rowe for help in the preparation of the manuscript.

References

Andrews TJ, Halpern SD, Purves D. Correlated size variations in human visual cortex, lateral geniculate nucleus, and optic tract. J Neurosci 1997; 17: 2859–68.

Beck RW, Trobe JD, Moke PS, Gal RL, Xing D, Bhatti MT, et al. High- and low-risk profiles for the development of multiple sclerosis within 10 years after optic neuritis: experience of the optic neuritis treatment trial. Arch Ophthalmol 2003; 121: 944–9.

Brusa A, Jones SJ, Kapoor R, Miller DH, Plant GT. Long-term recovery and fellow eye deterioration after optic neuritis, determined by serial visual evoked potentials. J Neurol 1999; 246: 776–82.

Brusa A, Jones SJ, Plant GT. Long-term remyelination after optic neuritis: a 2-year visual evoked potential and psychophysical serial study. Brain 2001; 124: 468–79.

Chen W, Kato T, Zhu XH, Strupp J, Ogawa S, Ugurbil K. Mapping of lateral geniculate nucleus activation during visual stimulation in human brain using fMRI. Magn Reson Med 1998; 39: 89–96.

Chen W, Zhu XH, Thulborn KR, Ugurbil K. Retinotopic mapping of lateral geniculate nucleus in humans using functional magnetic resonance imaging. Proc Natl Acad Sci USA 1999; 96: 2430–4.

Confavreux C, Vukusic S, Moreau T, Adeleine P. Relapses and progression of disability in multiple sclerosis. N Engl J Med 2000; 343: 1430–8.

Eickhoff SB, Stephan KE, Mohlberg H, Grefkes C, Fink GR, Amunts K, et al. A new SPM toolbox for combining probabilistic cytoarchitectonic maps and functional imaging data. Neuroimage 2005; 25: 1325–35.

Faro SH, Mohamed FB, Tracy JI, Elfont RM, Pinus AB, Lublin FD, et al. Quantitative functional MR imaging of the visual cortex at 1.5 T as a function of luminance contrast in healthy volunteers and patients with multiple sclerosis. AJNR Am J Neuroradiol 2002; 23: 59–65.

Frederiksen JL, Petrera J. Serial visual evoked potentials in 90 untreated patients with acute optic neuritis. Survey Ophthalmol 1999; 44: S54–62.

Frederiksen JL, Larsson HB, Olesen J, Stigsby B. MRI, VEP, SEP and biothesiometry suggest monosymptomatic acute optic neuritis to be a first manifestation of multiple sclerosis. Acta Neurol Scand 1991; 83: 343–50.

Gareau PJ, Gati JS, Menon RS, Lee D, Rice G, Mitchell JR, et al. Reduced visual evoked responses in multiple sclerosis patients with optic neuritis: comparison of functional magnetic resonance imaging and visual evoked potentials. Mult Scler 1999; 5: 161–4.

Ghezzi A, Martinelli V, Torri V, Zaffaroni M, Rodegher M, Comi G, et al. Long-term follow-up of isolated optic neuritis: the risk of developing multiple sclerosis, its outcome, and the prognostic role of paraclinical tests. J Neurol 1999; 246: 770–5.

Halliday AM, McDonald WI, Mushin J. Delayed visual evoked response in optic neuritis. Lancet 1972; 1: 982–5.

Hickman SJ, Brex PA, Brierley CM, Silver NC, Barker GJ, Scolding NJ, et al. Detection of optic nerve atrophy following a single episode of unilateral optic neuritis by MRI using a fat-saturated short-echo fast FLAIR sequence. Neuroradiology 2001; 43: 123–8.

Hickman SJ, Toosy AT, Jones SJ, Altmann DR, Miszkiel KA, MacManus DG, et al. A serial MRI study following optic nerve mean area in acute optic neuritis. Brain 2004; 127: 2498–505.

Hickman SJ, Wheeler-Kingshott CA, Jones SJ, Miszkiel KA, Barker GJ, Plant GT, et al. Optic nerve diffusion measurement from diffusion--weighted imaging in optic neuritis. AJNR Am J Neuroradiol 2005; 26: 951–6.

Horton JC, Landau K, Maeder P, Hoyt WF. Magnetic resonance imaging of the human lateral geniculate body. Arch Neurol 1990; 47: 1201–6.

Iwasawa T, Matoba H, Ogi A, Kurihara H, Saito K, Yoshida T, et al. Diffusion-weighted imaging of the human optic nerve: a new approach to evaluate optic neuritis in multiple sclerosis. Magn Reson Med 1997; 38: 484–91.

Jones SJ. Visual evoked potentials after optic neuritis. Effect of time interval, age and disease dissemination. J Neurol 1993; 240: 489–94.

Kastner S, O'Connor DH, Fukui MM, Fehd HM, Herwig U, Pinsk MA. Functional imaging of the human lateral geniculate nucleus and pulvinar. J Neurophysiol 2004; 91: 438–48.

Langkilde AR, Frederiksen JL, Rostrup E, Larsson HB. Functional MRI of the visual cortex and visual testing in patients with previous optic neuritis. Eur J Neurol 2002; 9: 277–86.

Levin N, Orlov T, Dotan S, Zohary E. Normal and abnormal fMRI activation patterns in the visual cortex after recovery from optic neuritis. Neuroimage 2006; 33(4): 1161–8.

Lund TE, Madsen KH, Sidaros K, Luo WL, Nichols TE. Non-white noise in fMRI: does modelling have an impact? Neuroimage 2006; 29: 54–66.

McAlonan K, Cavanaugh J, Wurtz RH. Attentional modulation of thalamic reticular neurons. J Neurosci 2006; 26: 4444–50.

Miki A, Liu GT, Modestino EJ, Liu CSJ, Englander SA, Haselgrove JC. Functional magnetic resonance imaging of lateral geniculate nucleus and visual cortex at 4 Tesla in a patient with homonymous hemianopia. Neuro Ophthalmol 2001; 25: 109–14.

Miki A, Liu GT, Goldsmith ZG, Liu CS, Haselgrove JC. Decreased activation of the lateral geniculate nucleus in a patient with anisometropic amblyopia demonstrated by functional magnetic resonance imaging. Ophthalmologica 2003; 217: 365–9.

Miki A, Liu GT, Modestino EJ, Bonhomme GR, Liu CS, Haselgrove JC. Decreased lateral geniculate nucleus activation in retrogeniculate hemianopia demonstrated by functional magnetic resonance imaging at 4 Tesla. Ophthalmologica 2005; 219: 11–5.

Miller NR. Walsh and Hoyt's clinical neuro-ophthalmology. 4th edn. Baltimore: Williams and Wilkins; 1982. p. 69–86.

Nilsson P, Larsson EM, Maly-Sundgren P, Perfekt R, Sandberg-Wollheim M. Predicting the outcome of optic neuritis: evaluation of risk factors after 30 years of follow-up. J Neurol 2005; 252: 396–402.

O'Connor DH, Fukui MM, Pinsk MA, Kastner S. Attention modulates responses in the human lateral geniculate nucleus. Nat Neurosci 2002; 5: 1203–9.

Ogawa S, Lee TM, Kay AR, Tank DW. Brain magnetic resonance imaging with contrast dependent on blood oxygenation. Proc Natl Acad Sci USA 1990; 87: 9868–72.

Pantano P, Mainero C, Iannetti GD, Caramia F, Di Legge S, Piattella MC, et al. Contribution of corticospinal tract damage to cortical motor reorganization after a single clinical attack of multiple sclerosis. Neuroimage 2002; 17: 1837–43.

Pantano P, Mainero C, Lenzi D, Caramia F, Iannetti GD, Piattella MC, et al. A longitudinal fMRI study on motor activity in patients with multiple sclerosis. Brain 2005; 128: 2146–53.

Rocca MA, Mezzapesa DM, Falini A, Ghezzi A, Martinelli V, Scotti G, et al. Evidence for axonal pathology and adaptive cortical reorganization in patients at presentation with clinically isolated syndromes suggestive of multiple sclerosis. Neuroimage 2003; 18: 847–55.

Rombouts SA, Lazeron RH, Scheltens P, Uitdehaag BM, Sprenger M, Valk J, et al. Visual activation patterns in patients with optic neuritis: an fMRI pilot study. Neurology 1998; 50: 1896–9.

Russ MO, Cleff U, Lanfermann H, Schalnus R, Enzensberger W, Kleinschmidt A. Functional magnetic resonance imaging in acute unilateral optic neuritis. J Neuroimaging 2002; 12: 339–50.

Saeki N, Fujimoto N, Kubota M, Yamaura A. MR demonstration of partial lesions of the lateral geniculate body and its functional intra-nuclear topography. Clin Neurol Neurosurg 2003; 106: 28–32.

Schneider KA, Richter MC, Kastner S. Retinotopic organization and functional subdivisions of the human lateral geniculate nucleus: a high-resolution functional magnetic resonance imaging study. J Neurosci 2004; 24: 8975–85.

Sherman SM. Thalamic relays and cortical functioning. Prog Brain Res 2005; 149: 107–26.

Slotnick SD, Klein SA, Carney T, Sutter EE. Electrophysiological estimate of human cortical magnification. Clin Neurophysiol 2001; 112: 1349–56.

Smith KJ, McDonald WI. The pathophysiology of multiple sclerosis: the mechanisms underlying the production of symptoms and the natural history of the disease. Philos Trans R Soc Lond B Biol Sci 1999; 354: 1649–73.

Sorensen TL, Frederiksen JL, Bronnum-Hansen H, Petersen HC. Optic neuritis as onset manifestation of multiple sclerosis: a nationwide, long-term survey. Neurology 1999; 53: 473.

Tamraz J. Neuroradiologic investigation of the visual system using magnetic resonance imaging. J Clin Neurophysiol 1994; 11: 500–18.

Toosy AT, Hickman SJ, Miszkiel KA, Jones SJ, Plant GT, Altmann DR, et al. Adaptive cortical plasticity in higher visual areas after acute optic neuritis. Ann Neurol 2005; 57: 622–33.

Toosy AT, Werring DJ, Bullmore ET, Plant GT, Barker GJ, Miller DH, et al. Functional magnetic resonance imaging of the cortical response to photic stimulation in humans following optic neuritis recovery. Neurosci Lett 2002; 330: 255–9.

Trip SA, Schlottmann PG, Jones SJ, Li WY, Garway-Heath DF, Thompson AJ, et al. Optic nerve atrophy and retinal nerve fibre layer thinning following optic neuritis: evidence that axonal loss is a substrate of MRI-detected atrophy. Neuroimage 2006a; 31: 286–93.

Trip SA, Wheeler-Kingshott C, Jones SJ, Li WY, Barker GJ, Thompson AJ, et al. Optic nerve diffusion tensor imaging in optic neuritis. Neuroimage 2006b; 30: 498–505.

Werring DJ, Bullmore ET, Toosy AT, Miller DH, Barker GJ, MacManus DG, et al. Recovery from optic neuritis is associated with a change in the distribution of cerebral response to visual stimulation: a functional magnetic resonance imaging study. J Neurol Neurosurg Psychiatry 2000; 68: 441–9.

Wohlschlager AM, Specht K, Lie C, Mohlberg H, Wohlschlager A, Bente K, et al. Linking retinotopic fMRI mapping and anatomical probability maps of human occipital areas V1 and V2. Neuroimage 2005; 26: 73–82.

Youl BD, Turano G, Miller DH, Towell AD, MacManus DG, Moore SG, et al. The pathophysiology of acute optic neuritis. An association of gadolinium leakage with clinical and electrophysiological deficits. Brain 1991; 114: 2437–50.